# CAMD for Entrainer Screening of Extractive Distillation Process Based on New Thermodynamic Criteria

Ivonne Rodriguez-Donis, Xinqiang You, Nataliya Shcherbakova, Vincent Gerbaud, Jens Abildskov, Stefano Cignitti

# CAMD for Entrainer Screening of Extractive Distillation Process Based on New Thermodynamic Criteria

Stefano Cignitti[a], Ivonne Rodriguez-Donis[b]*, Jens Abildskov[a], Xinqiang You[c], Nataliya Shcherbakova[d], Vincent Gerbaud[d],

[a]PROSYS, Department of Chemical and Biochemical Engineering, Technical University of Denmark, Denmark
[b]Laboratoire de Chimie Agro-Industrielle, Université de Toulouse, INRA, INP, Toulouse, France
[c]State Key laboratory of Chemical Engineering and Department of Chemistry, East China University of Science and Technology, Shanghai 200237, China
[d]Laboratoire de Génie Chimique, Université de Toulouse, CNRS, INP, UPS Toulouse, France
ivonne.rodriguezdonis@ensiacet.fr

This paper presents a framework for finding homogeneous entrainers E to separate non-ideal mixtures AB by extractive distillation. The framework is a systematic approach to convert a Computer Aided Molecular Design into a mixed integer non-linear program (MINLP). It is based on the thermodynamic properties of binary mixtures AE and BE and of isovolatility curve maps of the ternary mixture ABE. Entrainer candidates are ranked by the maximization of the driving force of A and B in their respective mixtures AE and BE as well as by minimizing the entrainer composition $x_E$ corresponding to a fixed value of the relative volatility $\alpha_{AB}$. The framework application is highlighted through an entrainer problem design for the separation of acetone – methanol by extractive distillation process.

## 1. Introduction

Extractive distillation is commonly used for the separation of non-ideal mixtures AB by adding an entrainer E that modifies the relative volatility of A or B enabling their separation. The entrainer determines the effectiveness of the process because it is strongly based on the thermodynamic properties of the ABE ternary residue curve maps (RCM) (Kiva et al., 2003). Unlike azeotropic distillation, the design of the extractive distillation process requires the extra knowledge of the location of the univolatility curve $\alpha_{AB}$. Indeed, the combined analysis of the RCM and the location of the curve $\alpha_{AB}=1$ allows defining which component A or B is the distillate product as well as the related extractive column configuration (Gerbaud and Rodriguez-Donis, 2014). A number of short-cut methods are available to design extractive distillation, but the selection of the entrainer is still mostly performed by computing the selectivity $S_{A,B}^{\infty E}$ and capacity $C_B^{\infty E}$ based on the activity coefficients of A and B at infinite dilution in the entrainer according to (Kossack et al., 2008):

$$S_{A,B}^{\infty E} * C_B^{\infty E} = \frac{\gamma_A^{\infty E}}{\gamma_B^{\infty E}} * \frac{1}{\gamma_B^{\infty E}} = \frac{\gamma_A^{\infty E}}{(\gamma_B^{\infty E})^2} \quad (1)$$

The entrainer screening based on $S_{A,B}^{\infty E}$ and $C_B^{\infty E}$ criteria finds good entrainers if the relative volatility $\alpha_{AB}$ increases monotonically with $x_E$ in ABE mixture reaching its maximum around the E apex. Further process optimization studies have contradicted the entrainer ranking by using these criteria. In the separation of acetone(A) – methanol(B), DMSO exhibited a lower $S_{A,B}^{\infty E}$ (1.47) and $C_B^{\infty E}$ (1.37) than water ($S_{A,B}^{\infty E}$=4.82, $C_B^{\infty E}$=2.1) but optimization studies performed by Kossack et al. (2008) verified that DMSO allowed the separation with a much lower total annual cost (TAC). Dissimilar to water where $\alpha_{AB}$ increases with $x_E$ in ABE mixture and reaches its maximum value around the water apex, DMSO has a lower $S_{A,B}^{\infty E}$ because the increasing of $\alpha_{AB}$ occurs at an intermediate value of $x_E$ in ABE mixture according to the isovolatility curve maps displayed in Figure 1.

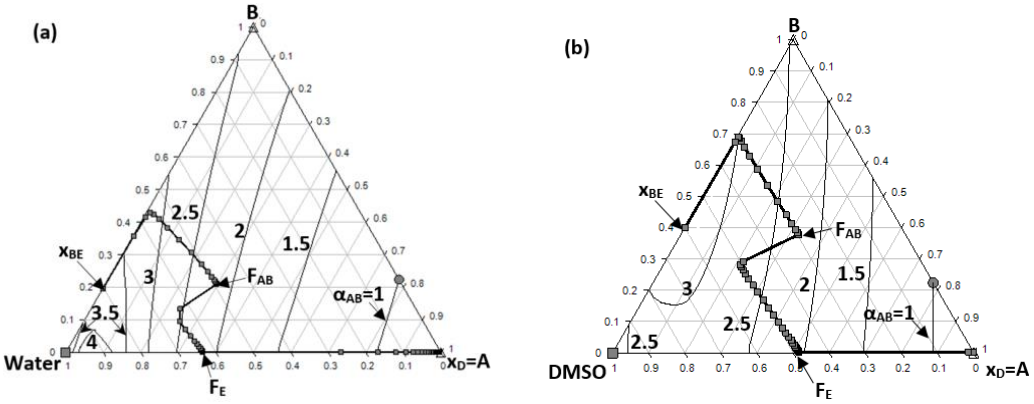


*Figure 1: Isovolatility curve maps for acetone(A) – methanol(B) using water (a) and DMSO (b) as entrainer.*

Figure 1 also displays the optimal liquid profile inside the extractive distillation column for DMSO and water. They are detailed later and were obtained by using ASPEN simulator built-in SQP method and following the methodology proposed by You et al. (2015a). In the case of DMSO, the intersection between the extractive and the rectifying liquid profile happens at $F_E$ with a lower $x_E$ as well as the stripping profile starting at $F_{AB}$ and moving towards $x_{BE}$. Hence, the separation of the bottom product $x_{BE}$ of the extractive column in a subsequent distillation column is easier because of the higher composition of methanol. You et al., (2015b) defined a separation efficiency indicator based on the difference of product content in $F_{AB}$ and $F_E$. It is higher here for DMSO that enhances product composition more effectively in the extractive section than water. But those authors concluded that maximizing only that indicator was not a suitable criterion. We extended our isovolatility curve maps analysis and process optimisation for all entrainers studied by Kossack et al. (2008), some providing acetone as distillate product in the extractive column and some providing methanol as distillate product, depending on the isovolatility curve direction towards A-E or B-E. A major breakthrough came from the combined analysis of the topology of the isovolatility curve maps and the driving force approach of Petersen and Gani (2004). The intersection between the rectifying and the extractive liquid profile at $F_E$ is located at the values of $x_E$ into the range of 0.5 to 0.7 where the $\alpha_{AB}$ usually varies between 1.5 and 2.5. Indeed, De Figueredo et al. (2015) pointed out that minimum TAC is mainly determined by the reflux ratio corresponding to an optimal location of $F_E$ in Figure 1 at $x_E$ between 0.2 and 0.7. We noticed that the increasing of the driving force of A and B in the respective mixture AE and BE is also associated with improved efficiency of the separation in the extractive column and in the subsequent solvent recovery column. Figure 2 displays the driving force of the mixtures AE and BE for water and DMSO. It suggests that DMSO is a better entrainer than water because the significant improvement of the driving force of acetone and methanol along with the lower $x_E$ of the intersection of the curves $\alpha_{AB}$=1 and $\alpha_{AB}$=2 on the AE edge (Figure 1). Therefore, these results suggest that these thermodynamic properties are more suitable for E screening than criteria based on $S_{A,B}^{\infty E}$ and $C_B^{\infty E}$ computations or other indicators.

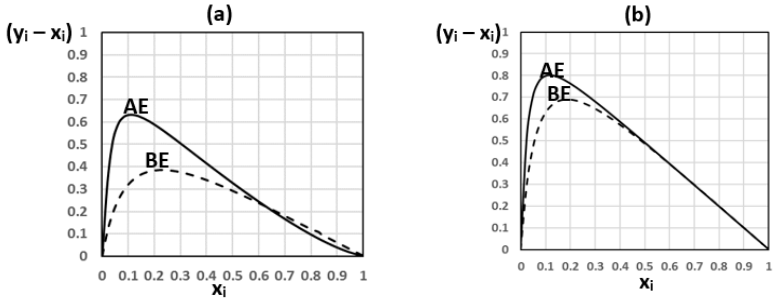


*Figure 2: Driving force of mixtures AE and BE for water(a) and DMSO(b) where i: A or B.*

This paper presents a framework for CAMD of pure homogeneous entrainer for extractive distillation processes. The entrainer screening is based on the driving force (DF) of the mixtures AE and BE and the composition of the entrainer $x_E$ at the intersection of the isovolatility curves $\alpha_{AB}$=1 and $\alpha_{AB}$=2 on the side AE (resp. BE) for A (resp. B) as distillate product of the extractive distillation column. The framework is a systematic approach to convert a CAMD problem into a mixed integer non-linear programming problem (MINLP). The framework application is highlighted through the entrainer design problem for the separation of the azeotropic binary mixture acetone – methanol by extractive distillation.

## 2. CAMD framework for design of homogeneous entrainer for extractive distillation process

The computer-aided framework for design of pure homogeneous entrainers for extractive distillation processes utilizes the needs and target properties to translate the CAMD problem into an MINLP formulation. The CAMD framework has four steps detailed here as adopted by Cignitti et al. (2018):

*Step 1: Problem Definition*

The process needs and target properties of the entrainers are defined. These can be thermodynamic properties, economic, and environmental needs. The product type refers to the type of desired molecule, such as chain size, chain type (acyclic, cyclic, aromatic etc.), and type and occurrence of the functional groups. First, from the process nature, the process needs to separate A and B using two connected distillation columns. Depending on the entrainer A (or B) is the distillate in the extractive distillation column and B (or A) in the next solvent recovery column. Due to the complexity of handling both options at the same time, each alternative is considered separately. The entrainer is fully miscible with A and B and does not form azeotropes. Process energy requirements decrease by using an entrainer with a low boiling point and vaporization enthalpy.

*Step 2: CAMD Formulation*

Here, the needs are formulated through lower and upper bounds of the target properties. Only acyclic solvents containing C, H and/or O atoms are chosen for the sake of this case study. Thus, the group set $\upsilon$ only contains acyclic groups (see Eq. 3) containing C, H and/or atoms ($\upsilon \in$ {$CH_3$, $CH_2$, CH, C, OH, $CH_3OH$, CHO, $CH_3COO$, $CH_2COO$, HCOO, $CH_3CO$, $CH_2O$, HCO, COOH, COO}). The size of the generated solvents is limited and their respective lower and upper bounds given in Table 1. NG is the total number of groups and NF is the total number of functional groups. The need regarding an energy efficient solvent is expressed as a low boiling temperature ($T_b$) and vaporization enthalpy ($\Delta$H). Both pure properties are computed by group contribution method (GCM). The need of non-formation of binary azeotrope with A and B is verified through the computation of the distribution coefficient of E ($K_E$) for each AE and BE mixture according to the constraint (6). Complete miscibility of the entrainer with the components A and B is ensured by constraining the value and the respective second derivatives of Gibbs free energy of mixing (β and β') of the mixtures AE and BE, respectively, to positive values.

*Table 1: Lower and Upper bounds for specified process needs*

| **Product constraints** | | | | **Process constraints** | | | |
|---|---|---|---|---|---|---|---|
| Need | Lower | Upper | Constraint | Need | Lower | Upper | Constraint |
| $N_G$ | 3 | 6 | Eq.3 | $K_E$ | - | 1 | Eq.6 |
| Tb (K) | 373 | 473 | Eq.4 | $\beta_{AE}$ and $\beta_{BE}$ | - | 0 | Eq.7 |
| $\Delta H_{vb}$ (kJ/mol) | 65 | - | Eq.5 | $\beta'_{AE}$ and $\beta'_{BE}$ | 0 | - | Eq.8 |
| | | | | $x_E$ for $\alpha_{AB}$=1 | 0 | 0.2 | Eq.9 & Eq.11 |
| | | | | $x_E$ for $\alpha_{AB}$=2 | 0 | 0.7 | Eq.10 & Eq.11 |

As the objective function, the driving force (DF) of the binary mixture AE and BE should be maximized at the same time while the entrainer composition $x_E$ for the intersection of the isovolatility values $\alpha_{AB}$=1 and $\alpha_{AB}$=2 are considered as constraints. Equation (2) provided the mathematical formulation of the objective function according to the driving force definition proposed by Petersen and Gani (2004).

*Step 3: MINLP Formulation*

Based on CAMD formulation, the MINLP problem is written:

Max $F_{obj} = |y_A - x_A|_{AE} + |y_B - x_B|_{BE}$ (2)

s.t structural constraints:

$\sum_i \sum_j \upsilon_{i,j} (2 - v_j) = 2$ (3)

pure component property constraints: $g_2(\boldsymbol{N}) \leq 0$

$473 \leq 204.359 * log \sum_i N_i T_{bi}$ (4)

$65 \leq \Delta H_{vb0} + \sum_i N_i \Delta H_{vbi}$ (5)

thermodynamic model constraints: $g_3(\boldsymbol{X}, \boldsymbol{N}) \leq 0$

$\frac{\gamma_i * P_i^0}{P_T} \leq 0$ (6)

$\sum_i x_i * ln\gamma_i + \sum_i x_i * lnx_i \leq 0$ (7)

$0 \leq \frac{\partial^2 (\sum_i x_i * ln\gamma_i + \sum_i x_i * lnx_i)}{\partial x_i^2}$ (8)

$(P_A^O * \gamma_A^{A,E}) / (P_B^O * \gamma_B^{\infty A,E}) - 1 = 0$ (9)

$(P_A^O * \gamma_A^{A,E}) / (P_B^O * \gamma_B^{\infty A,E}) - 2 = 0$ (10)

$((1 - x_E) * P_A^O * \gamma_A^{A,E} + x_E * P_E^O * \gamma_E^{A,E} - P_T = 0$ (11)

Where "i" is A (resp. B) in the binary mixture AE (resp. BE), $\gamma$ is the activity coefficient computed from Original UNIFAC (1-parameter), $P^O$ is the vapour pressure computed from Antoine's equation and $P_T$ = 1 atm.

*Step 4: Solution of MINLP Problem*

In most CAMD problems including the evaluation of thermodynamic properties of mixtures, the need of using nonlinear property and process models can lead to non-convex and non-smooth problems, which are difficult to solve. The MINLP formulation is then solved through a simultaneous approach according to the method proposed by Cignitti et al. (2018).

## 3. Case study

This paper aims to design an entrainer for an extractive distillation process involving two connected continuous columns. Given the binary azeotropic mixture acetone(A) – methanol(B), find a suitable entrainer for separating acetone(A) in the extractive distillation column while the binary mixture methanol(B) – entrainer(E) is separated in the second distillation column. Feasible entrainers have to provide the intersection of the curve $\alpha_{AB}$=1 on the edge AE defining acetone as the most volatile component inside the resulting ternary RCM (Gerbaud and Rodriguez-Donis, 2014). Molecular structures of entrainer candidates can be designed by maximizing the objective function according to equation (2). Solution of the MINLP problem through a simultaneous approach yields the ethylene glycol as a promising entrainer candidate for separating acetone – methanol by extractive distillation process. Kossack et al. (2008) included ethylene glycol in their screening of entrainers by using the $S_{A,B}^{\infty E}$ criterion computed by using Original UNIFAC or UNIQUAC model with binary coefficients available in ASPEN. $S_{A,B}^{\infty E}$ was 1.5 times higher when using the UNIQUAC model. Indeed, the topology of the isovolatility curve maps of ethylene glycol with Original UNIFAC is similar to that for DMSO (Figure 1b). The relative volatility $\alpha_{AB}$ reaches its maximum value at an entrainer composition around 0.7 (Figure 3a).

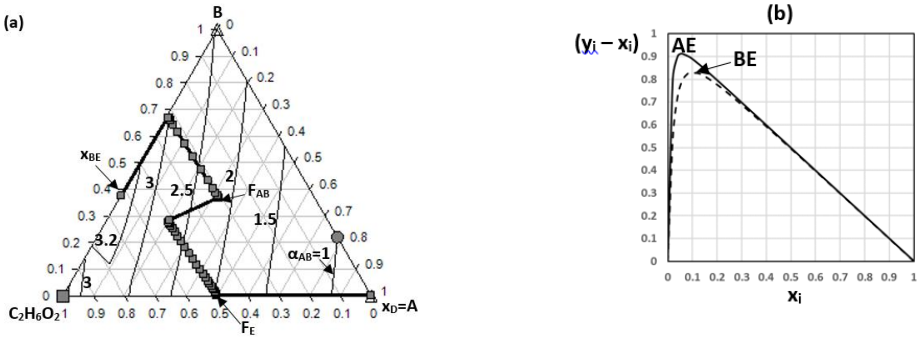


*Figure 3: (a) Isovolatility curve maps for acetone(A) – methanol(B) – ethylene glycol(E). (b) Driving force curves for the mixtures AE and BE where i: A or B.*

Table 2 displays physical properties for standard solvents like water and DMSO and those computed for ethylene glycol. The maximum value of the driving force (DF) for the respective binary mixtures AE and BE as well as the entrainer composition for a given relative volatility is also reported in Table 2.

*Table 2: Comparison of the optimal design entrainer with benchmark solvents*

| Optimal Solvent | $T_b$ (K) | $\Delta H$ (kJ/mol) | $K_E^{AE}$ | $K_E^{BE}$ | $\beta_E^{AE}$ | $\beta_E^{BE}$ | $DF_{AE}$ | $DF_{BE}$ | $x_E$ $\alpha_{AB}=1$ | $x_E$ $\alpha_{AB}=2$ |
|---|---|---|---|---|---|---|---|---|---|---|
| water | 273 | 40.8 | <1 | <1 | >0 | >0 | 0.6308 | 0.3843 | 0.172 | 0.6 |
| DMSO | 462 | 43.8 | <1 | <1 | >0 | >0 | 0.8016 | 0.6883 | 0.115 | 0.471 |
| $C_2H_6O_2$ | 470 | 64.5 | <1 | <1 | >0 | >0 | 0.9104 | 0.8284 | 0.129 | 0.511 |

Figure 3b shows the driving force of the binary mixture AE and BE for ethylene glycol. It can be compared with those of water and DMSO shown in Figure 2. Ethylene glycol increases significantly the driving force of acetone and methanol for their respective binary mixture AE and BE facilitating the separation of acetone mainly in the rectifying section of the extractive distillation column and methanol in the subsequent distillation column. Moreover, the intersection of the isovolatility curves $\alpha_{AB}$=1 and $\alpha_{AB}$=2 takes place at the edge AE with a similar entrainer composition $x_E$ to those computed for DMSO according to Table 2. DMSO and ethylene glycol have much better values of these thermodynamic criteria than water and comparable performances could be expected for both entrainers. However, ethylene glycol has a greater boiling temperature and vaporization enthalpy than water and DMSO. These properties will have a major negative impact on the energy consumption

and the total annual cost of the resulting extractive distillation process. Pre-design superiority of ethylene glycol over the standard entrainers as water and DMSO must be confirmed by comparison of the three entrainers based on optimization studies. In the case of water, the optimization study was carried out by You et al. (2015a) enhancing the previous results obtained for Luyben (2008) by defining a new energy related objective function OFE where the MINLP problem was solved through a two level strategy. First, the Aspen simulator Built-in SQP method is used for minimizing the OFE under fixed purity and recovery constraints as well as column configurations. Second, a sensitivity analysis was carried out for further minimization of OFE by adjusting the distillate flow rate, the total number of tray and the feed location for both columns. The same methodology was used for determining the optimal operating conditions for DMSO and ethylene glycol. Table 3 displays the optimization results while Figures 1a, 1b and 3a display the optimal liquid profiles into the extractive distillation column for water, DMSO and ethylene glycol, respectively. These figures show that the optimal extractive liquid profile starts at $F_E$ with a $x_E$ composition greater for DMSO and ethylene glycol enabling the separation with lower energy consumption (OFE) and TAC. Moreover, the extractive liquid profile is located in a region of isovolatility values between 2 and 2.5 for the three entrainers.

*Table 3 : Optimized values of the operating conditions for water, DMSO and ethylene glycol*

| Entrainers | Water | | DMSO | | Ethylene glycol | |
|---|---|---|---|---|---|---|
| Parameters | Extractive column | Second Column | Extractive column | Second Column | Extractive column | Second Column |
| Total trays | 82 | 26 | 41 | 13 | 58 | 7 |
| Rectifying trays | 37 | 16 | 2 | 4 | 2 | 3 |
| Extractive trays | 28 | - | 24 | - | 26 | - |
| Stripping trays | 15 | 8 | 13 | 7 | 28 | 2 |
| $F_E$ (kmol/h) | 844.8 | - | 402.8 | - | 445.6 | - |
| Reflux ratio | 2.46 | 1.3 | 1.408 | 0.09 | 1.448 | 0.05 |
| D (kmol/h) | 271 | 271.1 | 270.5 | 270.5 | 270.3 | 270.2 |
| $Q_{condenser}$ (MW) | 7.702 | 6.095 | 5.361 | 2.937 | 5.442 | 2.815 |
| $Q_{Reboiler}$ (MW) | 8.825 | 6.195 | 6.88 | 4.318 | 6.901 | 4.75 |
| TAC ($10^6$\$) | 4.348 (+31.4%) | | 3.309 (0%) | | 3.398 (+2.8%) | |
| OFE (kJ/kmol) | 29816.9 (+34.5%) | | 22164.1 (0%) | | 23054.7 (+4.0%) | |

According to the results in Table 3, DMSO provides the separation of acetone – methanol with lower energy consumption and lower total annual cost (TAC), beating ethylene glycol by a few percent, which was the preferred choice from the CAMD step based on the increase of the driving force (DF) for A and B. The higher DF of acetone and methanol facilitates essentially the separation of acetone in the rectifying section of the extractive column and the methanol in the second distillation column. Nevertheless, a competitive phenomenon must occur inside the extractive and the stripping section of the extractive column. Hence, the optimal separation of A and B in the entire extractive column is related to a suitable difference between the maximum value of DF for AE and BE mixtures. Although one could define a criterion based on the ratio between the DF of A in AE to B in BE, it requires more extensive optimization studies including a large variety of cases study. Figure 4 displays the optimal liquid profile in both the extractive column and the solvent recovery distillation column along with the DF curves of AE and BE. Figure 4 shows that the position of the liquid profile in the extractive section (between $F_E$ and $F_{AB}$) is located in a region where the DF of acetone is slightly greater for ethylene glycol than DMSO and much greater than water. We also notice that DMSO and ethylene glycol require similar reflux ratio and number of equilibrium trays in the extractive section. Actually, the separation of the components takes place under a more constant value of driving force value compared to water. In the case of ethylene glycol, the stripping section entails a higher tray number because of the smaller difference between the DF curves of A and B in the respective AE and BE mixtures. However, the solvent recovery column accomplishes the separation of methanol with a lower tray number and very small reflux ratio for ethylene glycol. Indeed, the liquid profile in the second recovery column is located in a region with a slightly better DF for methanol (see Figure 4). It should be noted that the feed position $F_{BE}$ in the solvent recovery column is not at the maximum value of DF of the BE curves because the optimal operation conditions are computed considering both columns together. As it was expected from results of Table 2, the entrainer flow rate for DMSO and ethylene glycol are comparable due to the similar $x_E$ values for $\alpha_{AB}$=1 and $\alpha_{AB}$=2. The main drawback of using ethylene glycol lies on the high boiling temperature and the vaporization enthalpy demanding a greater heat duty $Q_{reboiler}$ in the solvent recovery column. In conclusion, the screening of entrainers based on the computation of the driving force for components A and B along with the closer position of the isovolatility curves to the apex of the distillate component provide more

suitable optimal candidates than the use of criterion based on the computation of activity coefficients at infinite dilution in the entrainer.

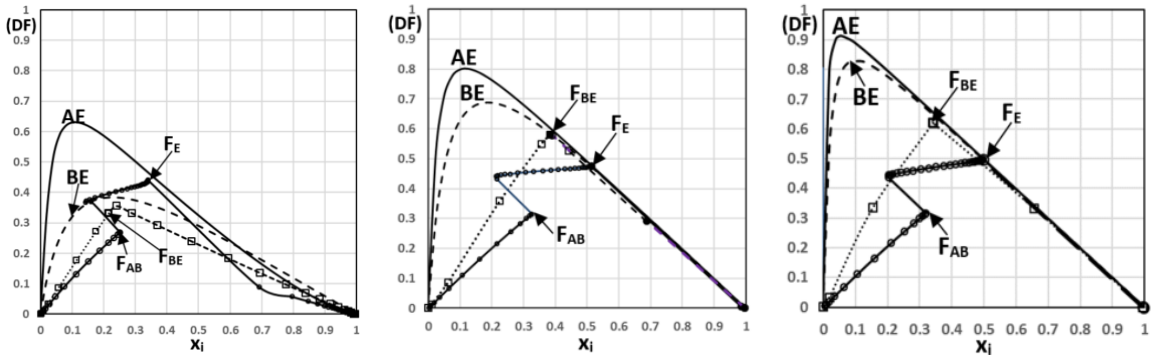


*Figure 4: Optimal liquid profile into the extractive distillation column and the solvent recovery column along with driven force curves for water (left), DMSO (center), ethylene glycol (right); where i: acetone or methanol*

## 4. Conclusions

This paper presents a framework for computer-aided molecular design (CAMD) of a pure homogeneous entrainer E for separating non-ideal AB mixtures by extractive distillation. The framework is a systematic approach to convert a CAMD problem into a mixed integer non-linear programming problem. The screening of optimal entrainers is based on new thermodynamic criteria involving the maximization of the driving force (DF) of the binary mixtures AE and BE as well as a low entrainer composition $x_E$ for the isovolatility curves $\alpha_{AB}=1$ and $\alpha_{AB}=1$. Ethylene glycol was obtained as a promising entrainer displaying a similar isovolatility curves chart than DMSO but enhancing the DF of acetone (A) and methanol (B). High DF of the BE mixture allows the separation separating in the solvent recovery column with a lower tray number and reflux ratio. However, an optimal DF ratio of AE and BE may exist for a selective separation of the distillate product into the extractive and the stripping section of the extractive distillation column. Optimization studies demonstrated that the entrainer screening based on the computation of the driving force and the entrainer composition at fixed isovolatility curves provide a much better fit to the optimization results in order to set the final extractive distillation process. Candidates from applying these criteria allows the separation of the components with low entrainer flow rate, reflux ratio and equilibrium trays number. However, energy related properties as boiling temperature and vaporization enthalpy must also be considered due to their negative effect on the total annual cost.

### References


Bek-Pedersen E., Gani R., 2004, Design and synthesis of distillation systems using a driving-force-based approach, Chemical Engineering & Processing, 43, 251–262.

Cignitti S., Mansouri S.S., Woodley J. M., Abildskov J., 2018, Systematic optimization-based integrated chemical product–process design framework, Industrial & Engineering Chemistry Research, 57, 677–688.

Gerbaud V., Rodriguez-Donis I., 2014, Extractive distillation, Chapter 6, Distillation: equipment and processes. Ed. Gorak, A. Olujic, Z., Elsevier, Amsterdam, 201-246.

De Figueiredo M.F., Brito K.D., Ramos W.B., Vasconcelos L.G.S., Brito R.P., 2015, Effect of solvent content on the separation and the energy consumption of extractive distillation columns. Chemical Engineering Communications, 202, 1191–1199.

Kiva V.N, Hilmen E.K., Skogestad S., 2003, Azeotropic phase equilibrium diagrams: a survey. Chemical Engineering Science, vol. 58, 1903-1953.

Kossack S., Kraemer K., Gani R., Marquardt W., 2008, A Systematic Synthesis Framework for Extractive Distillation Processes, Chemical Engineering Research & Design, Vol. 86, 781-792.

Luyben W.L., 2008, Comparison of Extractive Distillation and Pressure-swing Distillation for Acetone − Methanol Separation, Industrial and Engineering Chemistry Research, 47, 2696-2707

You X., Rodriguez-Donis I., Gerbaud V., 2015 a, Improved design and efficiency of the extractive distillation process for acetone-methanol with water, Industrial and Engineering Chemistry Research, 54, 491-501.

You X., Rodriguez-Donis I., Gerbaud V., 2015 b, Investigation of separation efficiency indicator for the optimization of the acetone-methanol extractive distillation with water. Industrial and Engineering Chemistry Research, 54, 10863-10875.